J. Plasma Physics (2004), *vol.* 70, *part* 6, *pp.* 651–669.
DOI: 10.1017/S0022377804003046 Printed in the United Kingdom

Local analysis of MHD spectra for cylindrical plasmas with flows

CHUNMEI WANG, J.W.S. BLOKLAND, R. KEPPENS and J.P. GOEDBLOED

FOM-Institute for Plasma Physics 'Rijnhuizen', Association EURATOM/FOM, Trilateral Euregio Cluster, PO Box 1207, 3430 BE, Nieuwegein, The Netherlands (chunmei@rijnh.nl)

(Received 6 January 2004 and in revised form 17 March 2004)

Abstract. An analytical and numerical study of the ideal magnetohydrodynamic (MHD) spectrum of waves and instabilities of a cylindrical plasma column with flows is presented. Our analytical results are relevant for thermally stratified, rotating, magnetized cylindrical equilibria. The presence of azimuthal flow makes the general analysis of the MHD spectrum difficult, except in cases where the continuous parts of the spectrum are absent. In the presence of Doppler shifted Alfvén and slow continua, a local analysis at resonant surfaces or internal extrema can provide a simple and reliable way to access information on MHD spectroscopy. In this paper, local cluster conditions, which govern the occurrence of sequences of discrete global modes, have been generalized for rotating equilibria. The generalized Suydam criterion for instability is revisited. A numerical study confirms our analytical results and clearly demonstrates how the local criteria govern the existence of the accumulating eigenmodes.

1. Introduction

The magnetohydrodynamic (MHD) description of plasma motion assumes that the constituent electron and ions species can be treated as fluids and that the dynamics of interest are at the macroscopic length and time scales. Specifically, MHD focuses on lengths much larger than ion cyclotron radii, and time scales longer than the inverse ion cyclotron frequencies $\omega_{\rm ic}^{-1}$. For plasma dynamics on time scales shorter than the resistive decay of the magnetic field, the ideal single fluid MHD description is appropriate. Since ideal MHDs express basic conservation laws (mass, momentum, energy, and magnetic flux) directly generalizing the Euler equations of compressible gas dynamics, much theoretical understanding of macroscopic plasma behavior has been developed within the ideal MHD framework. In particular, to analyze the stability properties of a given static (no flow) equilibrium configuration, one can exploit either the energy variational principle (Newcomb 1960), or directly solve the linearized MHD equations by analytic or numerical means. The possibility to use the knowledge on all waves and instabilities specific to a given equilibrium state as a diagnostic on the equilibrium itself has been termed as MHD spectroscopy (Goedbloed et al. 1993). This encompasses computing the MHD spectrum of all stable and unstable modes for the configuration at hand: when there are no unstable modes, the eigenfrequencies and eigenoscillations can still be used as

a 'magnetoseismological' means to probe the equilibrium structure. This has met significant successes in various solar physics applications, from active region or sunspot seismology (Bogdan and Braun 1995) to coronal seismology (Nakariakov et al. 1999) of loops and magnetic arcades in the solar corona.

The MHD spectrum of a plasma in equilibrium is governed by the equation of motion, typically written in terms of the Lagrangian displacement field $\boldsymbol{\xi}$ of a fluid element. In a static equilibrium, this equation of motion is

$$\rho \partial^2 \boldsymbol{\xi} / \partial t^2 = \mathbf{F}_{\mathrm{static}}(\boldsymbol{\xi}), \tag{1.1}$$

which contains the self-adjoint force operator $\mathbf{F}_{\mathrm{static}}(\boldsymbol{\xi})$ ($\mathbf{F}_{\mathrm{static}}$ is self-adjoint, if $\int \boldsymbol{\eta}^* \cdot \mathbf{F}_{\mathrm{static}}(\boldsymbol{\xi})\, d\mathbf{r} = \int \mathbf{F}_{\mathrm{static}}(\boldsymbol{\eta})^* \cdot \boldsymbol{\xi}\, d\mathbf{r}$ for arbitrary vectors $\boldsymbol{\xi}$ and $\boldsymbol{\eta}$), and its eigenvalues ω, from $\boldsymbol{\xi} \sim e^{-i\omega t}$, can only be real or purely imaginary (Bernstein et al. 1958). Sufficient and necessary conditions for stability can equivalently be obtained by exploiting the energy principle, which shows that static inhomogeneous MHD equilibria can be unstable due to pressure gradients or equilibrium current densities. However, the force operator formalism allows one to compute the complete ideal MHD spectrum, which for a one-dimensional (1D) static plasma column consists of unstable discrete modes, stable discrete modes, and stable continuous spectra. The latter are the Alfvén and slow continua and form the basic organizing structure of the MHD spectrum (Goedbloed and Poedts 2004). The discrete parts of the spectra can split into five Sturmian or anti-Sturmian (the number of zeros of the radial eigenfunction ξ is a monotonically increasing (Sturmian) or decreasing (anti-Sturmian) function of ω^2) sequences of sub-spectra separated by the Alfvén (ω_{A}^2) and slow (ω_{S}^2) continua, and two additional spectral ranges where monotonicity does not hold in general. Infinite sequences of discrete global modes can cluster at the tips of the Alfvén or the slow continua once local cluster conditions are satisfied (Goedbloed and Sakanaka 1974), also giving rise to the so-called global Alfvén eigenmodes (Appert et al. 1982). These modes were also studied by Mahajan et al. (1983) with the additional effect of a finite ion cyclotron term $\omega/\omega_{\mathrm{ic}}$.

In contrast to static plasma equilibria, where a detailed picture has been established for the stability of a cylindrical plasma configuration, it is still a challenge to make sense of the complete MHD spectrum of waves and instabilities for equilibria with both axial and azimuthal flow. This is in essence due to the loss of the self-adjointness property of the governing force operator. The study of MHD spectra with flows has already attracted a lot of attention (Spies 1978; Hameiri 1981). At the present time, the MHD stability of rotating geometrically confined plasmas has become a question of practical importance, for example in fusion research because of substantial neutral beam power in recent tokamak experiments, available not only to heat the plasma, but also to produce mass flows (Brau et al. 1983; Burrell et al. 1988). Furthermore, plasma flows are ubiquitous in astrophysical contexts, such as magnetized accretion disks, collimated jets and stellar winds. These flows have speeds which substantially influence the background equilibrium state, and therefore its stability against small perturbations.

In our previous paper (Wang et al. 2003), we studied the MHD stability of a slow capillary discharge for laser wakefield accelerator applications ignoring the background flow field. In the present paper, we analytically and numerically study the ideal MHD spectrum for a rotating magnetized plasma in such a cylindrical column. Although the introduction of equilibrium flows destroys the self-adjointness of the force operator, within ideal MHDs we still retain the basic structure of the full MHD

spectrum organized around the stable slow and Alfvén continua and the fast cluster points. In the presence of flow, we now distinguish between backward and forward Alfvén and slow continua. Note that for static equilibria, the introduction of non-ideal effects like resistivity not only makes the eigenproblem no longer self-adjoint, but significantly changes the entire MHD spectrum: the ideal, stable continua are replaced by a dense collection of damped, discrete modes located on specific curves in the complex eigenfrequency plane (Lortz and Spies 1984; Pao and Kerner 1985). In this paper, we avoid this additional complication and conveniently exploit the fact that we can still unambiguously identify the stable continua.

We focus primarily on local characteristics, deriving the conditions for the existence of cluster sequences at internal extrema of the forward and backward Alfvén continua $\Omega_{\rm A}^{\pm}$ and slow continua $\Omega_{\rm S}^{\pm}$ (defined later in (2.18) and (2.19)). This generalizes the earlier work of Bondeson et al. (1987) by the inclusion of plasma rotation. Our numerical results confirm the appearance and disappearance of cluster sequences as governed by the analytical cluster conditions. As in Bondeson et al. (1987), we treat axial and azimuthal flows in the generalized Hain–Lüst equation, and recover the generalized Suydam criterion at the resonant surface, where $\mathbf{k}_0\cdot\mathbf{B}=0$ with $\mathbf{k}_0\equiv(0,m/r,k)$. In general, sequences of damped and overstable interchange modes locally accumulate in oscillation frequency to the value of the Doppler shift $\mathbf{k}_0\cdot\mathbf{v}$, once this generalized Suydam criterion is satisfied. However, when a local extremum in the continua $\Omega_{\rm A}^{\pm}$, $\Omega_{\rm S}^{\pm}$ passes through the resonant surface, we always find unstable modes, which no longer strictly obey the analytical cluster conditions or Suydam's criterion.

This paper is arranged as follows. In Sec. 2, starting from the Frieman–Rotenberg equation of motion, the second-order eigenvalue problem is derived. In Sec. 3, we recover the sufficient and necessary stability criterion for the magnetized Couette flow against axisymmetric perturbations recently derived by means of the interchange method (Christodoulou et al. 2003). We also present the generalized Suydam criterion and the local cluster conditions valid at the internal extrema of the continua. In Sec. 4, the numerical solutions consider the effects of azimuthal flow on clustering, in contrast to part of the analysis and the numerical examples shown in Bondeson et al. (1987), which solely accounted for axial flow in the equilibrium.

2. Eigenvalue problem

To study the MHD spectrum in the presence of equilibrium flows, we begin with the basic formalism introduced by Frieman and Rotenberg (1960):

$$\rho\frac{\partial^2\boldsymbol{\xi}}{\partial t^2}+2\rho\mathbf{v}\cdot\nabla\frac{\partial\boldsymbol{\xi}}{\partial t}-\mathbf{F}(\boldsymbol{\xi})=0, \tag{2.1}$$

where

$$\mathbf{F}(\boldsymbol{\xi})=\mathbf{F}_{\rm static}(\boldsymbol{\xi})+\nabla\cdot[\rho\boldsymbol{\xi}(\mathbf{v}\cdot\nabla)\mathbf{v}-\rho\mathbf{v}\mathbf{v}\cdot\nabla\boldsymbol{\xi}], \tag{2.2}$$

$$\mathbf{F}_{\rm static}(\boldsymbol{\xi})\equiv-\nabla\Pi+\mathbf{B}\cdot\nabla\mathbf{Q}+\mathbf{Q}\cdot\nabla\mathbf{B}, \tag{2.3}$$

with the Eulerian perturbations of the total pressure Π and the magnetic field $\mathbf{Q}$

$$\Pi=-\boldsymbol{\xi}\cdot\nabla p-\gamma p\nabla\cdot\boldsymbol{\xi}+\mathbf{B}\cdot\mathbf{Q}, \tag{2.4}$$

$$\mathbf{Q}=\nabla\times(\boldsymbol{\xi}\times\mathbf{B}). \tag{2.5}$$

https://doi.org/10.1017/S0022377804003046 Published online by Cambridge University Press

The variables ρ, $\mathbf{v}$, $\mathbf{B}$ and p are the equilibrium density, plasma flow, magnetic field and thermal pressure, respectively. We adopt standard cylindrical coordinates (r, θ, z) and assume that all equilibrium variables only depend on the radial coordinate r (so that $v_r = B_r = 0$). All remaining equilibrium variables are then only constrained by the force balance in the radial direction:

$$\left(p + \frac{1}{2}B^2\right)' = \rho\frac{v_\theta^2}{r} - \frac{B_\theta^2}{r}, \tag{2.6}$$

where the prime denotes differentiation with respect to r. Note that the axial flow profile v_z is completely free. Because of the symmetry of the equilibrium, we consider the solutions of (2.1) in the form of normal modes:

$$\boldsymbol{\xi}(r, \theta, z, t) = (\xi_{r,mk}(r), \xi_{\theta,mk}(r), \xi_{z,mk}(r)) \exp i(m\theta + kz - \omega t). \tag{2.7}$$

It is instructive to use a field line projection which introduces the basic variables $\chi = r\xi_r$, $\eta = ir(\mathbf{B}/B) \times \mathbf{e}_r \cdot \boldsymbol{\xi}$ and $\zeta = ir\mathbf{B}/B \cdot \boldsymbol{\xi}$. Then after some algebra, the equation of motion (2.1) can be turned into a pair of first-order differential equations for χ and the perturbed total pressure Π:

$$\frac{AS}{r}\begin{pmatrix}\chi' \\ \Pi'\end{pmatrix} + \begin{pmatrix}C & D \\ E & -C\end{pmatrix}\begin{pmatrix}\chi \\ \Pi\end{pmatrix} = 0. \tag{2.8}$$

Here the coefficients are given by:

$$A = \rho\tilde{\omega}^2 - F^2 = \rho(\tilde{\omega} - \omega_{\mathrm{A}})(\tilde{\omega} + \omega_{\mathrm{A}}), \tag{2.9}$$

$$S = (\gamma p + B^2)\rho\tilde{\omega}^2 - \gamma p F^2 = \rho(\gamma p + B^2)(\tilde{\omega} - \omega_{\mathrm{S}})(\tilde{\omega} + \omega_{\mathrm{S}}), \tag{2.10}$$

$$C = -\frac{1}{r^2}\left[\left(B_\theta^2 - \rho v_\theta^2\right)\tilde{\omega}^2 + (B_\theta\tilde{\omega} + v_\theta F)^2\right]\rho\tilde{\omega}^2 + \frac{2m}{r^3}(B_\theta F + \rho v_\theta\tilde{\omega})S, \tag{2.11}$$

$$D = \rho^2\tilde{\omega}^4 - \left(k^2 + \frac{m^2}{r^2}\right)S, \tag{2.12}$$

$$E = -\frac{AS}{r^2}\left\{A + r\left[\frac{1}{r^2}\left(B_\theta^2 - \rho v_\theta^2\right)\right]'\right\} + \frac{4}{r^4}(B_\theta F + \rho v_\theta\tilde{\omega})^2 S$$

$$-\frac{1}{r^4}\left[\left(B_\theta^2 - \rho v_\theta^2\right)\rho\tilde{\omega}^2 + \rho(B_\theta\tilde{\omega} + v_\theta F)^2\right]^2, \tag{2.13}$$

where we introduce the local Doppler shifted frequency $\tilde{\omega} \equiv \omega - \mathbf{k}_0 \cdot \mathbf{v}$ with $\mathbf{k}_0 \equiv (0, m/r, k)$, the parallel gradient operator $F \equiv \mathbf{k}_0 \cdot \mathbf{B}$, the Alfvén frequency $\omega_{\mathrm{A}} \equiv F/\sqrt{\rho}$, the slow frequency $\omega_{\mathrm{S}} \equiv (F/\sqrt{\rho})\sqrt{\gamma p/(\gamma p + B^2)}$, and the ratio of specific heats γ. The system (2.8) was derived by Hameiri (1981) and Bondeson et al. (1987) for a cylindrical plasma with flow. Recently, a more general system for cases with equilibrium flow and radial gravitational stratification was obtained by Keppens et al. (2002), and used for MHD spectroscopy of accretion disks. One can use a generalization of the Hain–Lüst (1958) equation for flow:

$$\left(\frac{AS}{rD}\chi'\right)' + \left(U + \frac{V}{D} + \left(\frac{W}{D}\right)'\right)\chi = 0, \tag{2.14}$$

https://doi.org/10.1017/S0022377804003046 Published online by Cambridge University Press

which is equivalent to the system (2.8), where

$$U = \frac{A}{r} - \left[\frac{1}{r^2}\left(B_\theta^2 - \rho v_\theta^2\right)\right]', \tag{2.15}$$

$$V = -\frac{1}{r^3}\left(k^2 + \frac{m^2}{r^2}\right)\left[\left(2B_\theta^2 - \rho v_\theta^2\right)^2 \rho\tilde{\omega}^2 - \rho^2 v_\theta^2 (2B_\theta\tilde{\omega} + v_\theta F)^2\right]$$
$$- \frac{4}{r^3}(B_\theta F + \rho v_\theta \tilde{\omega})^2(\rho\tilde{\omega}^2 - k^2\gamma p) + \frac{4m}{r^4}(B_\theta F + \rho v_\theta\tilde{\omega})\left(2B_\theta^2 - \rho v_\theta^2\right)\rho\tilde{\omega}^2, \tag{2.16}$$

$$W = \frac{2S}{r^2}\left[kB_\theta G + \frac{m}{r}\rho v_\theta\tilde{\omega} + \rho v_\theta^2\left(k^2 + \frac{m^2}{r^2}\right)\right] - \frac{\rho^2 v_\theta\tilde{\omega}^2}{r^2}[2B_\theta F\tilde{\omega} + v_\theta(\rho\tilde{\omega}^2 + F^2)], \tag{2.17}$$

where $G = mB_z/r - kB_\theta$. Without flows ($\mathbf{v} = 0$, $\tilde{\omega} = \omega$), (2.14) reduces to the Hain–Lüst (1958) equation (i.e. Goedbloed's (1971) form of it for $\gamma \neq 1$). Equation (2.14) has singularities whenever $A = 0$ or $S = 0$. These singularities give rise to four continua, namely the forward and backward Alfvén continua

$$\Omega_{\mathrm{A}}^{\pm} \equiv \mathbf{k}_0 \cdot \mathbf{v} \pm \omega_{\mathrm{A}}, \tag{2.18}$$

and the forward and backward slow continua

$$\Omega_{\mathrm{S}}^{\pm} \equiv \mathbf{k}_0 \cdot \mathbf{v} \pm \omega_{\mathrm{S}}. \tag{2.19}$$

As clearly seen from the equivalent form (2.8), the frequency ranges given by $D = 0$ are not part of the MHD spectrum, so that these singularities of (2.14) are apparent (Appert et al. 1974).

For completeness, we point out that there is another continuum, with frequencies exactly given by the local Doppler shift $\Omega_{\mathrm{E}} \equiv \mathbf{k}_0 \cdot \mathbf{v}$, which is not described by the Lagrangian formalism exploited in (2.1), (2.8) or (2.14). This Eulerian entropy continuum does occur in all computations where spatially localized Eulerian perturbations are exploited (e.g. the set of primitive perturbed variables consisting of density ρ_1, velocity $\mathbf{v}_1$, pressure p_1, magnetic field $\mathbf{B}_1$). In particular, the numerical study of Sec. 4 is done in a Eulerian framework and the computed spectra will feature this additional continuum, as is pointed out there. The eigenmodes in this Eulerian entropy continuum represent trivial density or entropy disturbances, advected with the local flow speed. We directly derive all analytical results in the following from the Lagrangian description, safely ignoring this additional continuum. This is possible since all modes in this Eulerian entropy continuum are completely decoupled from the Alfvén, slow and fast MHD modes governed by (2.1), (2.8) or (2.14), and are therefore of marginal interest.

3. Analytical criteria for stability and clustering

Clearly much of the intricacy of the MHD spectroscopy of magnetized cylindrical plasma with flow hinges on the existence of the four stable continua $\Omega_{\mathrm{A}}^{\pm}$ and $\Omega_{\mathrm{S}}^{\pm}$. In general, due to the fact that these stable continua can partially overlap and/or have internal extrema, a complete stability assessment of a certain equilibrium needs a numerical approach. In some cases, it is possible to obtain local analytical criteria

https://doi.org/10.1017/S0022377804003046 Published online by Cambridge University Press

governing the existence of cluster sequences of discrete modes at surfaces where the local Alfvén/slow frequency vanishes or where an internal extremum is reached in one of the continua. In general, obtaining sufficient and necessary stability criteria is only possible for cases where the continua are absent. We first recover recent results on the stability of compressible magnetized Couette flow, independently obtained using the interchange method (Christodoulou et al. 1996) and the energy variational principle (Newcomb 1962).

3.1. *Stability criterion for magnetized Couette flow*

In the case of magnetized Couette flow ($v_z = 0$) and no axial magnetic field, the MHD continua vanish for perturbations that are axisymmetric ($m = 0$). Looking for solutions of (2.8), we can insert an oscillatory behavior $\exp(ik_r r)$ in the radial direction, where the radial wavelength should be much shorter than the typical length scale of the equilibrium variation, e.g. the cylinder radius R ($Rk_r \gg 1$). In this case, the 2×2 system (2.8) yields the local dispersion equation

$$k_r^2 \frac{A^2 S^2}{r^2} + C^2 + DE = 0. \tag{3.1}$$

For a *purely azimuthal magnetic field* and axisymmetric perturbations ($m = 0$), taking the limit $(k_r, k) \to \infty$ at finite ratio k_r/k, as in Keppens et al. (2002), and defining the fast magnetosonic speed $c_\theta^2 \equiv (\gamma p + B_\theta^2)/\rho$, the local dispersion equation (3.1) gives rise to solutions

$$\omega^2 \approx \frac{k^2}{k_r^2 + k^2} \left[-\frac{r}{\rho} \left(\frac{B_\theta^2}{r^2} \right)' + \frac{2 v_\theta (r v_\theta)'}{r^2} + \frac{\rho'}{\rho} \frac{v_\theta^2}{r} - \frac{\left(p_{\rm tot}' - B_\theta^2/r \right)^2}{c_\theta^2 \rho^2} \right], \tag{3.2}$$

where the total pressure $p_{\rm tot} \equiv p + B_\theta^2/2$. The term in square brackets then determines whether local unstable modes occur. In the hydrodynamic limit, the Solberg–Høiland criterion (Tassoul 1978) for stability is recovered since the positivity of this term can be written as

$$\kappa^2 + N^2 \geqslant 0, \tag{3.3}$$

where the Rayleigh term $\kappa^2 = 2 v_\theta (r v_\theta)'/r^2$ and the Brunt–Väisälä frequency $N^2 = [\rho'/\rho - p'/(\gamma p)] p'/\rho$.

The more general case of magnetized Couette flow was recently studied by Christodoulou et al. (2003). As is done there, we rewrite the stability expression in terms of certain physical quantities that are conserved during the interchange of two fluid elements. These are the specific angular momentum L ($\equiv r v_\theta = $ constant), the specific azimuthal magnetic flux Ψ ($\equiv B_\theta/(\rho r) = $ constant), and the specific entropy S ($\equiv p \rho^{-\gamma} = $ constant). So-called adiabatic changes in total pressure $p_{\rm tot}$ occur under the constraints of the conservation laws $\Psi = $ constant and $S = $ constant, so that

$$\left. \frac{dp_{\rm tot}}{dr} \right|_{\rm ad} = c_\theta^2 \frac{d\rho}{dr} + \frac{B_\theta^2}{r}. \tag{3.4}$$

We can then rewrite the term in square brackets in (3.2), yielding the necessary and sufficient condition for stability:

$$\frac{1}{r^3} \frac{dL^2}{dr} - \rho r \frac{d\Psi^2}{dr} - \frac{1}{\rho^2 c_\theta^2} \left(\frac{dp_{\rm tot}}{dr} - \frac{B_\theta^2}{r} \right) \left(\frac{dp_{\rm tot}}{dr} - \left. \frac{dp_{\rm tot}}{dr} \right|_{\rm ad} \right) \geqslant 0, \tag{3.5}$$

https://doi.org/10.1017/S0022377804003046 Published online by Cambridge University Press

exactly as obtained by Christodoulou et al. (2003) using the interchange method. They emphasized the importance of the coupling between magnetic tension and the total pressure gradient in the last magnetoconvective term of criterion (3.5).

For a system with *both azimuthal and axial magnetic fields* and axisymmetric perturbations, we consider the limit of long axial wavelength $k \to 0$, and $\mathbf{k}_0 \cdot \mathbf{B} \to 0$, which again makes the continua vanish. The local dispersion equation (3.1) then simplifies to

$$\omega^2 = k_r^2 \frac{\gamma p + B^2}{\rho} - \frac{r}{\rho}\left(\frac{B_\theta^2}{r^2}\right)' + \frac{2v_\theta (r v_\theta)'}{r^2} + \frac{\rho'}{\rho}\frac{v_\theta^2}{r}. \tag{3.6}$$

As pointed out by Christodoulou et al. (1996), the presence of B_z breaks the isolation of perturbations between axially separated regions, leading to non-conservation of the specific angular momentum L and specific azimuthal magnetic flux Ψ. The axial magnetic field introduces new conservation laws, namely the axial current I ($\equiv rB_\theta =$ constant), angular velocity Ω ($\equiv v_\theta/r =$ constant), specific axial magnetic flux H ($\equiv B_z/\rho =$ constant), and specific entropy S ($\equiv p\rho^{-\gamma} =$ constant) (Lubow and Spruit 1995; Christodoulou et al. 1996). If we adopt these conserved quantities, (3.6) transforms into

$$\omega^2 = r\frac{d\Omega^2}{dr} - \frac{1}{r^3\rho}\frac{dI^2}{dr} - \frac{1}{\rho^2 c_z^2}\left(\frac{dp_{\rm tot}}{dr} + \frac{B_\theta^2}{r}\right)\left(\frac{dp_{\rm tot}}{dr} - \left.\frac{dp_{\rm tot}}{dr}\right|_{\rm ad}\right)$$
$$+ k_r^2 c_B^2 + \frac{4B_\theta^2}{r^2\rho} + 4\Omega^2 + \frac{1}{\rho^2 c_z^2}\left(\frac{dp_{\rm tot}}{dr} + \frac{B_\theta^2}{r}\right)^2, \tag{3.7}$$

where $c_B^2 = (\gamma p + B^2)/\rho$, adiabatic changes in total pressure are now $dp_{\rm tot}/dr|_{\rm ad} = c_z^2\rho' - B_\theta^2/r$, and $c_z^2 = (\gamma p + B_z^2)/\rho$. Due to the positiveness of the last four terms, a sufficient criterion for stability is obtained:

$$r\frac{d\Omega^2}{dr} - \frac{1}{r^3\rho}\frac{dI^2}{dr} - \frac{1}{\rho^2 c_z^2}\left(\frac{dp_{\rm tot}}{dr} + \frac{B_\theta^2}{r}\right)\left(\frac{dp_{\rm tot}}{dr} - \left.\frac{dp_{\rm tot}}{dr}\right|_{\rm ad}\right) \geqslant 0, \tag{3.8}$$

in agreement with (32) of Christodoulou et al. (2003).

3.2. Generalized Suydam criterion

As is well known, in the absence of equilibrium flows, the violation of Suydam's criterion together with the validity of the oscillation theorem (Goedbloed and Sakanaka 1974) allow one to predict the existence of global instabilities. In fact, they would be the most global modes in the Sturmian sequence of unstable discrete modes accumulating to the marginal zero frequency. Hence, in the static case, the local Suydam criterion becomes a significant first test for overall stability. It also explicitly appears as such in Newcomb's (1960) stability theorems obtained from the ideal MHD energy principle. For the case of flowing equilibria studied here, although there is no counterpart to the energy principle, we state without proof that the oscillation theorem can be generalized to the case with flow for weakly inhomogeneous plasmas. This in turn makes the generalized Suydam criterion a useful tool in analyzing stability. However, a definitive conclusion on overall stability will require a full numerical treatment of the eigenvalue problem as well.

Hence, for more general cases than those studied in Sec. 3.1, where the continua $\Omega^{\pm}_{\mathrm{A,S}}$ do not vanish and equilibrium flow is involved, the lack of self-adjointness of the force operator in the linear MHD equation (2.1) prevents a stability determination by the energy principle. We can, however, still perform a local analysis at resonant surfaces ($F=0$), where the generalized Hain–Lüst equation (2.14) is singular for $\tilde{\omega}^2=0$.

Investigating the behaviour at such resonant surfaces separately still makes physical sense, since where $F=0$, perturbations do not disturb the equilibrium magnetic field locally. Hence, the driving forces of instability are minimally counterbalanced by magnetic tension, causing instabilities to be predominantly localized on this surface (Suydam 1958).

At a resonant surface $r=r_0$ where $\mathbf{k}_0\cdot\mathbf{B}=0$, both A and S vanish quadratically for a frequency equal to the local Doppler shift. We consider the situation $\tilde{\omega}(r_0)\pm\omega_{\mathrm{A,S}}(r_0)=0$, $(\tilde{\omega}\pm\omega_{\mathrm{A,S}})'(r_0)\neq 0$. Expansion of the coefficients A, S, D close to r_0 gives

$$A \approx F'^2(M^2-1)s^2, \tag{3.9}$$

$$S \approx (\gamma p+B^2)\big(M^2-M_c^2\big)F'^2 s^2, \tag{3.10}$$

$$D \approx \left(k^2+\frac{m^2}{r^2}\right)(\gamma p+B^2)F'^2\big(M^2-M_c^2\big)s^2, \tag{3.11}$$

where $s=r-r_0$, $M=-\sqrt{\rho}(\mathbf{k}_0\cdot\mathbf{v})'/(\mathbf{k}_0\cdot\mathbf{B})'$, and $M_c=\sqrt{\gamma p/(\gamma p+B^2)}$. Expanding U, V/D, and W/D in the same way and substituting all these terms back into the generalized Hain–Lüst equation (2.14) yields

$$(s^2\chi')'+D_0\chi=0, \tag{3.12}$$

where

$$D_0=\left(\frac{q}{q'B_z}\right)^2\frac{1}{1-M^2}\left\{-2\frac{p'}{r}-2\frac{B^2}{B_\theta^2}V_\theta\left(\frac{V_\theta}{r}\right)'-2\frac{V_\theta^2}{r^2}+2\frac{q'}{qr}\frac{B_z^2}{B_\theta}MV_\theta+\frac{1}{r^2B_\theta^2}\right.$$
$$\left.\times\frac{1-M_c^2}{(1-M^2)\big(M_c^2-M^2\big)}[(V_\theta+MB_\theta)^2+M^2\big(B_\theta^2-V_\theta^2\big)]^2+\frac{4(V_\theta+MB_\theta)^2}{r^2(1-M^2)}\right\}, \tag{3.13}$$

with $V_\theta=\sqrt{\rho}v_\theta$ and $q=rB_z/B_\theta$. These expressions were first published by Bondeson et al. (1987). Note that $D_0\to\pm\infty$ if M^2 approaches 1 or M_c^2. The first case occurs when the Alfvén frequency range $\Omega_{\mathrm{A}}(r)$ has a local extremum at r_0, while the second case indicates that the slow frequency range $\Omega_{\mathrm{S}}(r)$ has a local extremum at r_0. However, one should remember that the expression for D_0 obtained in (3.13) is based on the assumption $(\tilde{\omega}\pm\omega_{\mathrm{A,S}})'(r_0)\neq 0$, so that it is no longer valid when the local extremum of the Alfvén or slow continuum passes through r_0.

The behavior of χ close to the singularity is found from a Frobenius expansion:

$$\chi=s^\nu\sum_{n=0}^{\infty}a_n s^n. \tag{3.14}$$

For our purpose, it is sufficient to just determine the index ν from the leading order term $(\nu(\nu+1)+D_0)s^\nu$, which gives the indicial equation $\nu(\nu+1)+D_0=0$. The indicial equation has roots $\nu_{1,2}=-\frac{1}{2}\pm\sqrt{\frac{1}{4}-D_0}$, which are complex when

https://doi.org/10.1017/S0022377804003046 Published online by Cambridge University Press

$D_0 > \frac{1}{4}$. Consequently, the solutions χ oscillate infinitely rapidly as the singularity is approached, which signal the instabilities. This generalized Suydam criterion $D_0 > \frac{1}{4}$ provides an analytic condition for the existence of sequences of overstable and damped modes clustering towards the local Doppler shift. However, Suydam stability $D_0 < \frac{1}{4}$ does not guarantee that the equilibrium is globally stable (Sakanaka and Goedbloed 1974).

Equation (3.13) includes almost all local equilibrium variables and their local gradients, making it hard to deduce a clear physical interpretation. If we specialize to rigid rotation $v_\theta = \Omega r$ (where $\Omega =$ constant) and constant axial flow, so that $M = 0$, the criterion for stability reduces to

$$p' + \frac{r}{8}\left(\frac{q' B_z}{q}\right)^2 + \frac{B^2}{2B_\theta^2} r^2 \Omega^2 \rho' - \rho \Omega^2 r \left(\frac{B^2}{2B_\theta^2}\frac{\Omega^2 r^2}{c_{\rm s}^2} + 1\right) > 0, \tag{3.15}$$

where the sound speed $c_{\rm s} = \sqrt{\gamma p/\rho}$. Without rotation, (3.15) reduces to the well-known Suydam criterion (Suydam 1958), where the driving force of the instability is the pressure gradient in combination with the curvature of the magnetic field. From (3.15) one can see that rigid rotation without density variation ($\rho' = 0$) acts to locally destabilize the plasma. In combination with a density gradient, the centrifugal force with an unfavorable density gradient may destabilize the plasma, analogous to the Rayleigh–Taylor stability in a gravitational field, where the lighter fluid should sit on top of the heavier one for stability. The case of purely axial flow has already been presented in Bondeson et al. (1987, (8′)). For a plane-parallel, gravitationally stratified layer, the generalized Suydam criterion is found in van der Holst et al. (1999).

3.3. Local extrema in the continua and cluster conditions

The generalized Suydam criterion relies on the presence of a resonant surface where $F = 0$, and all four continua coincide. When such a resonant surface does not exist, cluster sequences of discrete global modes may still be associated with a local extremum in any of the forward and backward Alfvén continua $\Omega_{\rm A}^{\pm}$ or slow continua $\Omega_{\rm S}^{\pm}$.

When the *Alfvén continuum* $\Omega_{\rm A}^{\pm}$ *has a local extremum* at $r = r_{\rm A}^{\pm}$, we may consider frequencies in the neighborhood of that extremum so that $\tilde{\omega}(r_{\rm A}^{\pm}) \mp \omega_{\rm A}(r_{\rm A}^{\pm}) = 0$ and also $(\tilde{\omega} \mp \omega_A)'(r_{\rm A}^{\pm}) = 0$. We will assume $(\tilde{\omega} \mp \omega_{\rm A})''(r_{\rm A}^{\pm}) \neq 0$ though. The expansion of A close to $r_{\rm A}^{\pm}$ yields

$$A \approx \tfrac{1}{2} A'' s_{\rm A^{\pm}}^2 = \mp \rho \omega_{\rm A} \Omega_{\rm A}^{\pm\prime\prime} s_{\rm A^{\pm}}^2, \tag{3.16}$$

where $s_{\rm A^{\pm}} = r - r_{\rm A}^{\pm}$. Exploiting similar local expansions for the other coefficients S, D, U, V, and W, the generalized Hain–Lüst equation (2.9) reduces to

$$(s_{\rm A^{\pm}}^2 \chi')' + D_{\rm A}^{\pm} \chi = 0, \tag{3.17}$$

https://doi.org/10.1017/S0022377804003046 Published online by Cambridge University Press

where

$$D_{\rm A}^{\pm}=\frac{2}{A''}\left\{\frac{G^2r}{B^2}\left(\frac{2kB^2B_\theta}{r^2G}+\frac{B_\theta^2}{r^2}\right)'-\frac{4k^2B_\theta^2}{r^2}\left(1-\frac{\gamma p}{B^2}\right)+\frac{G^2r}{B^2}\left(\frac{V_\theta^2}{r^2}\pm\frac{2V_\theta FB_z}{r^2G}\right)'\right.$$
$$\left.\pm 8V_\theta\frac{kB_\theta(k\gamma p-B_zF)}{r^2B^2}-4V_\theta^2\left(\frac{k^2}{r^2}\left(1-\frac{\gamma p}{B^2}\right)+\frac{3kB_\theta G}{r^2B^2}\right)\mp 4V_\theta^3\frac{kG}{r^2B^2}\right\}, \tag{3.18}$$

with $A''=\mp 2\rho\omega_{\rm A}\Omega_{\rm A}^{\pm\prime\prime}$ from (3.15). Without rotation, $D_{\rm A}^{\pm}$ reduces to

$$D_{\rm A}^{\pm}=\frac{2}{A''}\left\{\frac{rG^2}{B^2}\left(\frac{2kB^2B_\theta}{r^2G}+\frac{B_\theta^2}{r^2}\right)'-\frac{4k^2B_\theta^2}{r^2}\left(1-\frac{\gamma p}{B^2}\right)\right\}, \tag{3.19}$$

which agrees with the expression given by Goedbloed (1984) and by Bondeson et al. (1987). Note that the local criterion is not influenced by axial flow.

As in the previous section, we exploit a Frobenius expansion about the singularity. The indicial equation $\nu(\nu+1)+D_{\rm A}^{\pm}=0$ is obtained from the leading order term, where the indices are $\nu_{1,2}=\frac{1}{2}\pm\sqrt{\frac{1}{4}-D_{\rm A}^{\pm}}$. If $D_{\rm A}^{\pm}>\frac{1}{4}$ is satisfied, there may exist sequences of modes clustering to the local extremum of the Alfvén continua $\Omega_{\rm A}^{\pm}$.

The same analysis can be carried out at an *internal extremum of the slow continua* $\Omega_{\rm S}^{\pm}$, considering frequencies in the neighborhood of that extremum so that $\tilde\omega(r_{\rm S}^{\pm})\pm\omega_S(r_{\rm S}^{\pm})=0$ and $(\tilde\omega\pm\omega_S)'(r_{\rm S}^{\pm})=0$. We assume $(\tilde\omega\pm\omega_S)''(r_{\rm S}^{\pm})\neq 0$ and expand S close to $r_{\rm S}^{\pm}$:

$$S\approx\tfrac{1}{2}S''s_{\rm S^{\pm}}^2=\mp\rho(\gamma p+B^2)\omega_{\rm S}\Omega_{\rm S}^{\pm\prime\prime}s_{\rm S^{\pm}}^2, \tag{3.20}$$

where $s_{\rm S^{\pm}}=r-r_{\rm S}^{\pm}$. We get the cluster condition $D_{\rm S}^{\pm}>\frac{1}{4}$ with

$$D_{\rm S}^{\pm}=\frac{2F^2}{S''}\frac{M_c^4}{1-M_c^2}\left\{F^2(1-M_c^2)+2B_\theta\left(\frac{B_\theta}{r}\right)'-\left(\frac{2B_\theta k}{rF}\right)^2(B^2+\gamma p)\right.$$
$$\pm r\left(\frac{2B_\theta V_\theta}{r^2M_c}\right)'+r\left(\frac{V_\theta^2}{r^2M_c^2}\right)'\pm\frac{8V_\theta B_\theta}{r^2F^2M_c}\left(kGB_\theta-k^2\gamma p\right)$$
$$+\frac{4V_\theta^2}{r^2F^2M_c^2}\left[F^2M_c^2-k^2\gamma p+\frac{m}{r}B_\theta F-2\left(k^2+\frac{m^2}{r^2}\right)B_\theta^2\right]$$
$$\left.\pm\frac{4V_\theta^3}{r^2F^2M_c}\left[\frac{m}{r}F-\left(k^2+\frac{m^2}{r^2}\right)\frac{B_\theta}{M_c^2}\right]-\frac{V_\theta^4(k^2+m^2/r^2)(1-M_c^2)}{r^2F^2M_c^4}\right\}, \tag{3.21}$$

where $S''=\mp 2\rho(\gamma p+B^2)\omega_{\rm S}\Omega_{\rm S}^{\pm\prime\prime}$ from (3.19). Note that as soon as rotation is included, both expressions (3.17) and (3.20) show a clear asymmetry between forward and backward shifted continua. Without azimuthal flow, (42) of Goedbloed (1984) or (31) of Bondeson et al. (1987) are recovered.

https://doi.org/10.1017/S0022377804003046 Published online by Cambridge University Press

4. Numerical study

For the numerical study of the MHD spectra of a cylindrical plasma column with flow, we exploit the code LEDAFLOW (Nijboer et al. 1997), which is a generalization of LEDA code (Kerner and Lerbinger 1985) for a one-dimensional equilibrium with flow. The MHD equations are linearized, a Fourier representation is used for the variation of the eigenfunctions in the homogeneous directions, and then they are discretized using finite elements in the inhomogeneous direction. A suitable combination of cubic Hermite elements and quadratic elements for the perturbed quantities prevents the creation of spurious eigenvalues. A Galerkin method is used to complete the system. The result is a complex non-Hermitian eigenvalue problem that is solved by a QR solver. The inverse vector iteration method is used to calculate the eigenfunctions for one single eigenvalue. The boundary conditions on the eigenfunctions treat the cylindrical edge as a rigid boundary.

4.1. Equilibrium

The following equilibrium is used in our numerical stability study:

$$\rho(r) = 1 + (D-1)r^2, \tag{4.1}$$

$$B_\theta(r) = \frac{1}{2} j_{z0} r \left(1 - \frac{\delta}{2} r^2\right), \tag{4.2}$$

$$B_z(r) = \sqrt{\frac{2}{\gamma \beta_0}} (1 - \Gamma r^2), \tag{4.3}$$

$$v_\theta(r) = r(A + Br + Cr^2), \tag{4.4}$$

where distances are normalized to the cylinder wall, $R = 1$. The density and the velocity are scaled with the density on the axis $\rho(0)$ and the sound speed on the axis $c_{s0} = \sqrt{\gamma p(0)/\rho(0)}$, respectively. In the equilibrium, $D \equiv \rho(1)/\rho(0)$ is the density variation. The azimuthal magnetic field is due to a diffuse current $j_z = j_{z0}(1 - \delta r^2)$. The parameter β_0 is the ratio of the thermal pressure to magnetic pressure on the axis, and Γ serves to quantify the cross-sectional variation of the longitudinal magnetic field. In (4.4), we have chosen a profile for v_θ that allows for easy manipulation of the location of a local extremum in the Alfvén and slow continua. Recently, a particular example of such a flow field vanishing at two concentric cylindrical boundaries (called a 'Dean flow') was applied by Huang and Hassam (2001) to a simple coil configuration for thermonuclear plasma confinement, where the centrifugal force should resolve the loss cone issue and the flow shear should stabilize interchanges. This would happen for supersonic flow speeds. Hence, we also allow for supersonic flow speeds but do not impose the Dean flow boundary conditions. Instead, we choose parameter values $A = 0, B \neq 0, C \neq 0$. This is slightly inconsistent on axis, but facilitates the best control of the localization of the modes. We will not consider axial flow; this was studied by Bondeson et al. (1987). The pressure is not treated as an independent variable, but is derived from the force balance equation (2.6).

In the following sections, we numerically solve the 1D linear MHD equations in cylindrical coordinates with the equilibrium profiles as specified above. Our simulations verify and extend the analytical results on how discrete modes accumulate to extrema in the continua, and Suydam modes oscillating at resonant surfaces.

https://doi.org/10.1017/S0022377804003046 Published online by Cambridge University Press

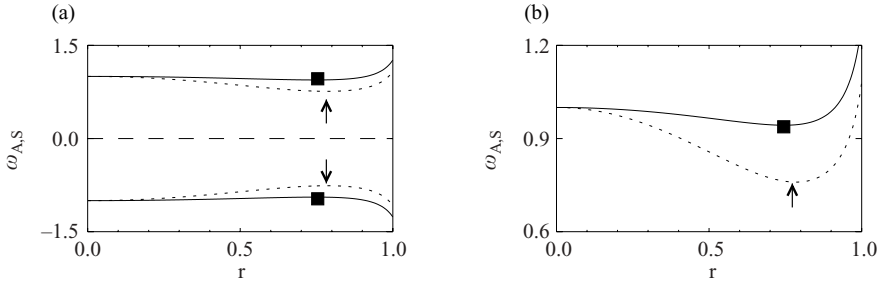

Figure 1. (a) Radial dependence of the Alfvén continua $\omega_A^{\pm}$ (full curves) and slow continua $\omega_S^{\pm}$ (dotted curves) for a static z-pinch equilibrium with $\beta_0^{-1}=0$, $D=0.1$, $j_{z0}=2.0$, $\delta=1.2$, and mode numbers $m=-1$, $k=2$. (b) Blow-up of the positive branches of the continua shown in (a). The arrows indicate the extrema which have cluster sequences, the squares indicate those that have no cluster sequences.

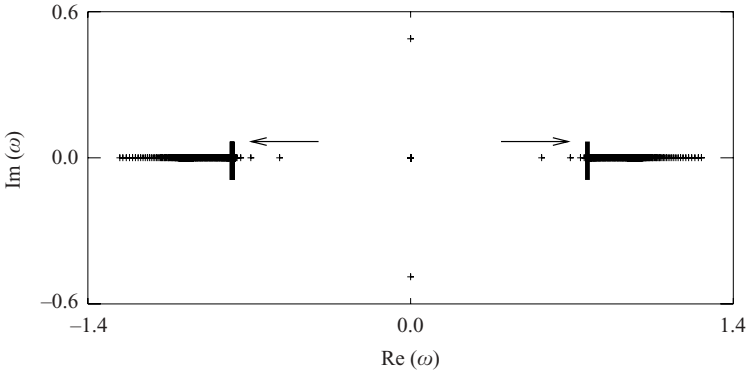

Figure 2. The entire MHD spectrum for the static z-pinch. Two sequences of discrete modes cluster to the extrema of ω_S^+ and ω_S^- marked by vertical bars. The arrows indicate the direction of an increasing number of nodes of the modes.

4.2. Cluster sequences

Beginning with a static case ($\Omega=0$), we consider a pure z-pinch ($\beta_0^{-1}=0$) with $D=0.1$, $j_{z0}=2.0$, $\delta=1.2$, and take mode numbers $m=-1$, $k=2$. Figure 1 shows the radial dependence of the Alfvén and slow continua, which have local extrema at $r=0.745$ and 0.785, respectively. At the local extrema of the Alfvén and slow continua, we obtain $D_A^{\pm}(0.745)=-12.4$, $D_S^{\pm}(0.785)=3.63$ (>0.25). The latter value forecasts that there may exist sequences of discrete global modes accumulating to the local extrema of $\omega_S^{\pm}$. The MHD spectra are presented in Fig. 2. In this figure, one clearly sees the unstable modes on the imaginary axis and the cluster sequences on the real axis at the edges of $\omega_S^{\pm}$. In this section, we focus on the cluster modes. To better understand the behavior of these modes, in Fig. 3 we present the axial velocity eigenfunction $v_{z,1}$ of the fifth cluster mode. Eigenfunctions of higher order modes show more oscillations when the singularity is approached, as expected by the oscillation theorem (Goedbloed and Sakanaka 1974).

https://doi.org/10.1017/S0022377804003046 Published online by Cambridge University Press

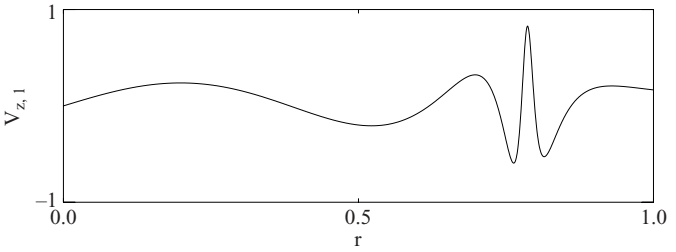

Figure 3. The eigenfunction $v_{z,1}$ of the fifth mode of Fig. 2, which oscillates most rapidly at the location of the extremum in the slow continuum at $r = 0.78$.

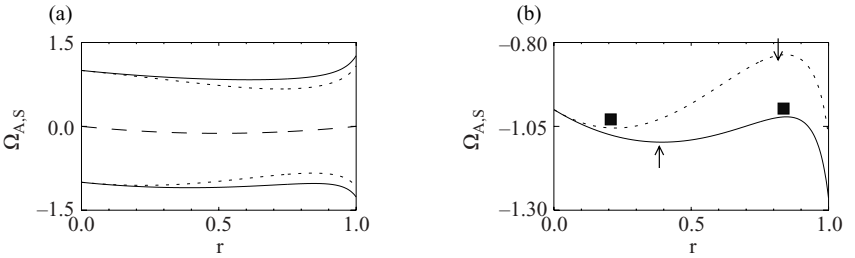

Figure 4. (a) Doppler shifted Alfvén continua $\Omega_{\rm A}^{\pm}$ (full curves) and slow continua $\Omega_{\rm S}^{\pm}$ (dotted curves) for an equilibrium with a 'Dean flow' $B = 0.5$, $C = -0.5$, corresponding a maximal Alfvén Mach number $M_{\rm A} \approx 0.13$, radial electric field $E_r = 0$, and other parameters as in Figs 1–3. The dashed curve is the local Doppler shift $\mathbf{k}_0 \cdot \mathbf{v}$. (b) Blow-up of the forward branches of the continua shown in (a). The arrows indicate the extrema which have cluster sequences, the squares indicate those that have no cluster sequences.

For identical density and magnetic equilibrium profiles, we now permit an azimuthal flow with $B = 0.5$, $C = -0.5$. For these parameter values, the azimuthal rotation reaches a maximal sonic Mach number $M_{\rm S} = v_\theta / c_{\rm s} \sim 0.08$ at a radial distance $r \approx 0.65$. Similarly, the Alfvén Mach number for the equilibrium rotation reaches $M_{\rm A} = v_\theta / (B_\theta / \sqrt{\rho}) \sim 0.13$ at $r \approx 0.5$. Due to the flow, the Alfvén and slow continua are no longer symmetric between backward and forward traveling modes (Fig. 4). The values of $D_{\rm A,S}^{\pm}$ at the internal extrema of the Alfvén and slow continua now become $D_{\rm S}^{+}(0.22) = -164.5$, $D_{\rm A}^{+}(0.39) = 89.4$ (>0.25), $D_{\rm S}^{+}(0.84) = 3.0$ (>0.25), $D_{\rm A}^{+}(0.85) = -5.4$, which are all associated with the forward continua $\Omega_{\rm A,S}^{+}$, and the remaining two $D_{\rm A}^{-}(0.61) = -14.9$, $D_{\rm S}^{-}(0.72) = 3.7$ (>0.25) are associated with the backward continua $\Omega_{\rm A,S}^{-}$. There are six extrema all together, three of which should have cluster sequences according to the criteria. In Fig. 5, which shows the computed spectrum, only two cluster sequences can be seen. Note that LEDAFLOW also computes the Eulerian entropy continuum, which coincides with the local Doppler shift $\mathbf{k}_0 \cdot \mathbf{v}$. It is situated around $\mathrm{Re}(\omega) = -0.1$ in Fig. 5. Comparing the spectrum with the continuous ranges plotted in Fig. 4, we find that the extremum of $\Omega_{\rm A}^{+}$ at $r = 0.39$ (which should have a cluster sequence) overlaps with the slow continuum at other positions. This superposition explains why we can no longer distinguish this cluster sequence. To make this sequence visible, we move the cylinder wall from $R = 1$ to 0.6, thereby eliminating the overlap with the slow

https://doi.org/10.1017/S0022377804003046 Published online by Cambridge University Press

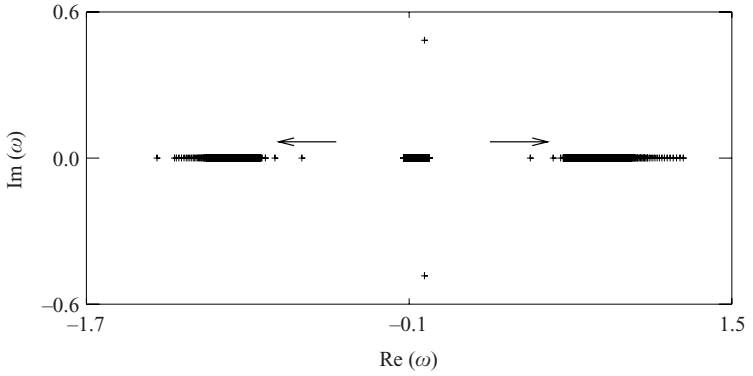

Figure 5. Entire MHD spectrum for $m=-1$, $k=2$, apparently only two sequences of discrete modes accumulating to the extrema of $\Omega_S^{\pm}$. A third predicted cluster sequence at Ω_A^+ is not distinguishable from that at Ω_S^+.

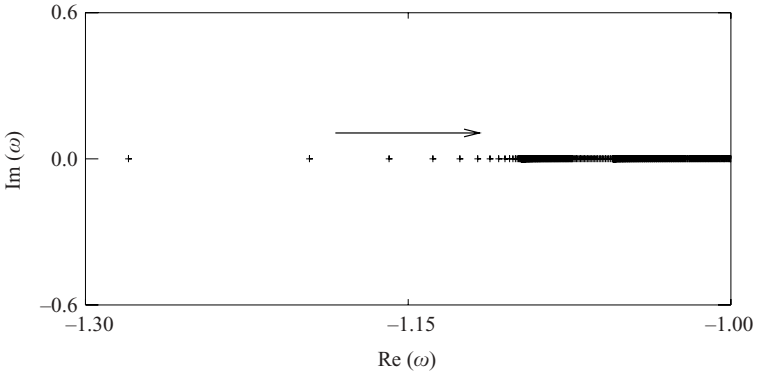

Figure 6. Part of the MHD spectrum for the equilibrium used in Figs 4 and 5, now restricted to the interval $0 \leqslant r \leqslant 0.6$. The 'missing' sequence of discrete modes clusters to the exposed edge of Ω_A^+ at $r=0.39$.

continuum. A part of the resulting MHD spectrum is shown in Fig. 6. As predicted analytically, we now see the third cluster sequence accumulating at the extremum of Ω_A^+ at $r=0.39$.

4.3. Suydam instability

The Suydam criterion is a necessary and sufficient condition for instability localized at a resonant surface. As mentioned by Goedbloed and Sakanaka (1974), in the static case, there are actually two numbers characterizing a Suydam eigenmode, namely, the number of nodes n in the radial direction and the azimuthal mode number m. High n or m modes are highly localized on this surface. The least localized mode is $m=1$, $n=0$, which is indeed the most unstable Suydam mode.

We now numerically explore the characteristics of the Suydam modes for a rotating plasma. We fix the mode numbers to $m=1$ and $k=1$, and consider a rotating equilibrium with parameters $D=1.0$, $j_{z0}=2.0$, $\delta=4.0$, $\beta_0^{-1}=1.5$, $\Gamma=1.8$,

https://doi.org/10.1017/S0022377804003046 Published online by Cambridge University Press

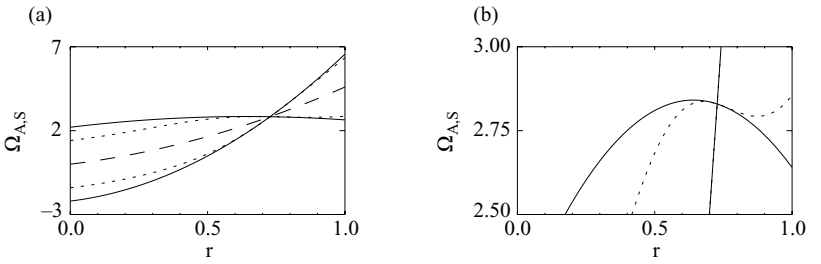

Figure 7. (a) Alfvén continua $\Omega_A^{\pm}$ (full curves), slow continua $\Omega_S^{\pm}$ (dotted curves), and Eulerian entropy continuum $\mathbf{k}_0 \cdot \mathbf{v}$ (dashed curve) for a rotating equilibrium with parameters $D = 1.0$, $j_{z0} = 2.0$, $\delta = 4.0$, $\beta_0^{-1} = 1.5$, $\Gamma = 1.8$, $B = 2.0$, $C = 2.6$, the mode numbers $m = 1$, $k = 1$, corresponding maximal Alfvén Mach number $M_A = 30$, and radial electric field E_r varying from -0.5 to 5. Note the presence of the resonant surface $\mathbf{k}_0 \cdot \mathbf{B} = 0$ at $r = 0.728$ where all continua coincide. (b) Blow-up of (a). Dropping the Eulerian entropy continuum, we clearly see the resonant surface and the nearby internal extrema.

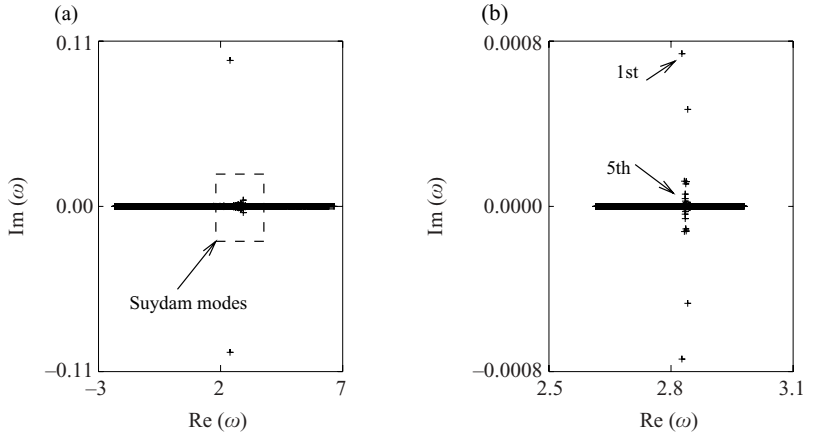

Figure 8. (a) The entire MHD spectrum for equilibrium parameters and mode numbers as in Fig. 7. The densely packed complex modes are closely related to the presence of the Suydam surface. (b) The MHD spectra with the same equilibrium, now restricted to the interval $0.71 \leqslant r \leqslant 0.74$.

$B = 2.0$, $C = 2.6$. Under these rather arbitrarily chosen parameter values, both B_θ and B_z change sign within the interval [0, 1], and the rotation becomes transonic at $r \approx 0.7$, reaching a Mach number $M_S \approx 1.7$ at $r = 1$. The rotation is also super-Alfvénic on a large part of the domain, reaching maximal Alfvén Mach number $M_A = 30$. Note that this equilibrium has a non-vanishing radial electric field E_r varying from -0.5 to 5 in dimensionless units. This choice of equilibrium parameters ensures that there is a resonant surface, as seen at $r = 0.728$ in Fig. 7(b), and at this surface $D_0 = 1.8 \times 10^3$. Figure 8(a) is the corresponding spectrum for this rotating system: two global complex modes coexist with a densely packed set of discrete local modes strongly relating to the Suydam surface. To better distinguish these local Suydam modes, we recompute the spectrum while restricting the equilibrium on a

https://doi.org/10.1017/S0022377804003046 Published online by Cambridge University Press

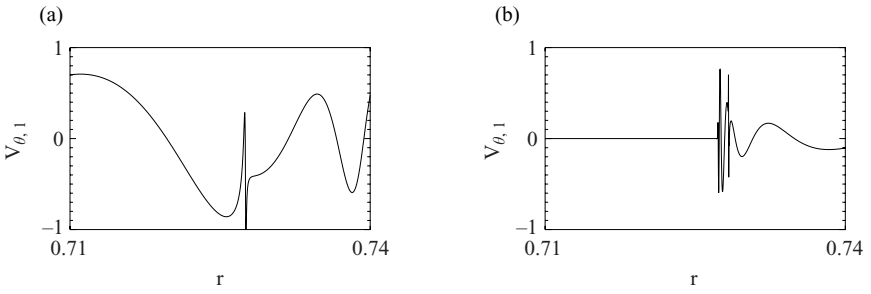

Figure 9. The azimuthal velocity eigenfunctions of the first mode (a) and the fifth mode (b) of Fig. 8(b). One can see that the eigenfunctions oscillate rapidly at the resonant surface $r = 0.728$.

small interval by setting an inner wall at $R_i = 0.71$ and the outer wall at $R_o = 0.74$. Figure 8(b) shows this MHD spectrum. The azimuthal velocity eigenfunctions $v_{\theta,1}$ of the first and the fifth modes from Fig. 8(b) are shown in Figs 9(a) and 9(b), respectively. In comparison to Fig. 9(a), one can see that the less unstable, higher order Suydam mode in Fig. 9(b) has more radial nodes and is more highly localized at the resonant surface.

As seen in Fig. 7(b), the continua not only have a resonant surface, but also have internal extrema. Motivated by the analogous study of the transition of local extrema through the resonant surface by Bondeson et al. (1987) for purely axial flow, we now carry out a similar study for a rotating plasma. Except for β_0, all the other parameters are set to be the same as in the case above. By varying β_0, the extremum of the slow continuum Ω_S^+ coincides with the resonant surface at the point $r_S = r_0 = 0.726$ with $\beta_0^{-1} = 1.008$. As explained before, the analytical formulae then diverge and $D_S^+ \to -\infty$, $D_0 \to +\infty$. We can move this extremum from the left of the resonant surface to the right of the resonant surface by further decreasing β_0^{-1}. Then, D_S and D_0 flip signs. This is also seen when numerically evaluating the data $D_S^+(0.726) = -4.7 \times 10^7$, $D_0(0.726) \to +\infty$ for $\beta_0^{-1} = 1.008$, and $D_S^+(0.730) = 1.2 \times 10^6$, $D_0(0.726) = -9.6 \times 10^8$ for $\beta_0^{-1} = 1.0$. Both D_S and D_0 tend to infinity and they have opposite signs for r_S close to r_0.

We have computed the complete spectrum for $\beta_0^{-1} = 1.008$ on the interval $0 \leqslant r \leqslant 1$ (Fig. 10(a)). As in Fig. 8(a), we find both global modes and local modes in the complex plane. To better understand the local modes, we focus on a small interval ($0.71 \leqslant r \leqslant 0.74$), again using 100 grid points (Fig. 10(b)). For much higher radial resolution, the figure does not change. According to the Suydam criterion or the cluster conditions, the complex modes of Fig. 10(b) closely relate to the Suydam surface and/or the extremum of Ω_S^+. However, unlike in Fig. 9(b), where the higher-order Suydam modes oscillate more rapidly at the resonant surface, this is not evident in the higher-order eigenfunctions in Fig. 11. The eigenfunctions vary globally with peaks at the resonant surface. When we slightly deviate r_S from r_0 by lowering $\beta_0^{-1} = 1.0$, the same conclusions can be drawn. The MHD spectra and eigenfunctions for $\beta_0^{-1} = 1.0$ and 1.008 are almost the same, as depicted in Figs 10 and 11. For these cases, we can no longer exploit the Suydam criterion and cluster conditions, as they are strictly speaking no longer valid for r_S very close to r_0.

https://doi.org/10.1017/S0022377804003046 Published online by Cambridge University Press

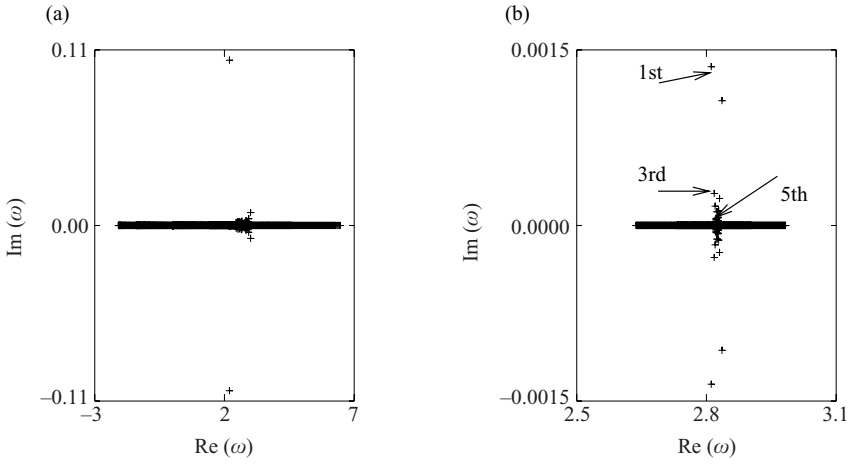

Figure 10. (a) The complete MHD spectrum on the interval $0 \leqslant r \leqslant 1$ and (b) on the interval $0.71 \leqslant r \leqslant 0.74$ for equilibrium parameters $D = 1.0$, $j_{z0} = 2.0$, $\delta = 4.0$, $\beta_0^{-1} = 1.008$, $\Gamma = 1.8$, $B = 2.0$, $C = 2.6$, and mode numbers $m = 1$, $k = 1$. The corresponding maximal Alfvén Mach number $M_A = 32$, and E_r varies from -4 to 0.5. When slightly varying β_0^{-1} from 1.008 to 1.0, D_0 flips sign from $+\infty$ to $-\infty$, while the MHD spectrum shows no pronounced difference.

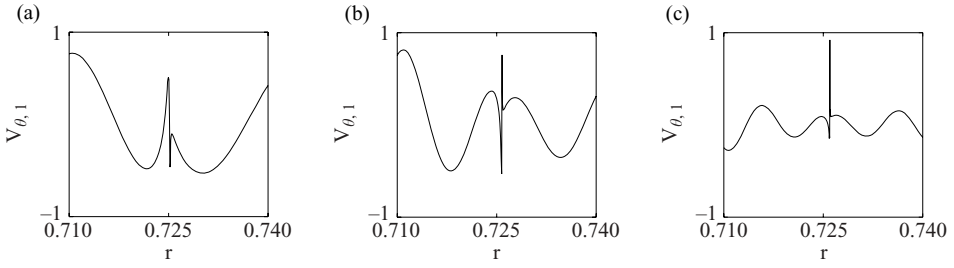

Figure 11. Azimuthal velocity eigenfunctions of (a) the first, (b) the third and (c) the fifth mode of Fig. 10(b).

5. Summary and discussion

In this paper we have performed an MHD spectroscopy study of a rotating magnetized plasma in a cylindrical column. We have generalized the analytical criteria which govern the existence of cluster sequences of discrete modes at surfaces where the local Alfvén/slow frequency vanishes or where an internal extremum is reached in one of the continua. Our numerical study included cases with and without rotation, and agrees well with the local cluster conditions. The generalized Suydam criterion was revisited and tested numerically with emphasis on the azimuthal equilibrium flow effects. The Suydam criterion provides a sufficient condition for instability when there is no extremum coincident with the resonant surface. However, when the extremum of the Alfvén or slow continua transit the resonant surface, our numerical study always shows instabilities that no longer strictly obey the analytical local Suydam criterion or cluster conditions.

Our analytical results are relevant for all thermally stratified, rotating, magnetized cylindrical equilibria. The presence of axial and azimuthal flows in the

https://doi.org/10.1017/S0022377804003046 Published online by Cambridge University Press

equilibrium clearly affects the overall MHD stability, as well as the appearance of sequences of discrete modes. Currently, virtually all practical applications of MHD spectroscopy ignore equilibrium flows altogether. For example, the observed oscillations of solar coronal loops have recently been interpreted as global kink modes with oscillation frequencies in the range of the ideal Alfvén continuum (Goossens et al. 2002), modeling the loop as a static cylindrical flux tube. A numerical study like that presented in Sec. 4 should be undertaken for stationary coronal loop equilibria. Similarly, in fusion plasmas, the occurrence of toroidal and poloidal flows can dramatically enrich the linear wave properties of the confined plasma. The assumption of a cylindrical plasma column ultimately needs to be relaxed for realistic aspect ratio tokamak configurations, where the effects of genuine toroidicity enter. In that context, first insights have emerged from studies where only toroidal equilibrium flow was taken into account, predicting the existence of global toroidal flow induced Alfvén eigenmodes (van der Holst et al. 2000). When poloidal flow is taken along as well, it enters the computation of the stationary toroidal equilibrium itself in a non-trivial manner (Beliën et al. 2002). Still within the ideal MHD framework, such stationary toroidal equilibria were then recently shown to allow for unstable Alfvén continuum modes when the equilibrium poloidal flow surpasses the slow magnetosonic speed (Goedbloed et al. 2004). Future work should investigate the generalizations of these ideal, single fluid MHD results on waves and instabilities in rotating plasmas, to more realistic, non-ideal, two-fluid models of plasma dynamics, where specifically the singular nature of the local continuum modes is likely to be replaced by finite amplitude behavior.

Acknowledgements

This work was performed as part of the research program of 'Stichting voor Fundamenteel Onderzoek der Materie' (FOM) with financial support from NWO, within the FOM programme 55 on Laser Wakefield Accelerators. R. Keppens and J. P. Goedbloed performed this work while supported by the European Communities under the contract of Association between EURATOM/FOM, carried out within the framework of the European Fusion Program. Views and opinions expressed herein do not necessarily reflect those of the European Commission.

References

Appert, K., Gruber, R. and Vaclavik, J. 1974 *Phys. Fluids* **17**, 1471.

Appert, K., Gruber, R., Troyon, F. and Vaclavik, J. 1982 *Plasma Phys.* **24**, 1147.

Beliën, A. J. C., Botchev, M. A., Goedbloed, J. P., van der Holst, B. and Keppens, R. 2002 *J. Comput. Phys.* **182**, 91.

Bernstein, I. B., Frieman, E. A., Kruskal, M. D. and Kulsrud, R. M. 1958 *Proc. Roy. Soc.* **A244**, 17.

Bogdan, T. J. and Braun, D. C. 1995 *Proc. 4th SOHO Workshop*, ESA SP-376, 31.

Bondeson, A., Iacono, R. and Bhattacharjee, A. 1987 *Phys. Fluids* **30**, 2167.

Brau, K., Bitter, M., Goldston, R. J., Manos, D., McGuire, K. and Suckewer, S. 1983 *Nucl. Fusion* **23**, 1643.

Burrell, K. H., Groebner, R. J., Stjohn, H. and Seraydarian, R. P. 1988 *Nucl. Fusion* **28**, 3.

Christodoulou, D. M., Contopoulos, J. and Kazanas, D. 1996 *ApJ* **462**, 865.

Christodoulou, D. M., Contopoulos, J. and Kazanas, D. 2003 *ApJ* **586**, 372.

Frieman, E. and Rotenberg, M. 1960 *Rev. Mod. Phys.* **32**, 898.

Goedbloed, J. P. 1971 *Physica* **53**, 501.

Goedbloed, J. P., Holties, H. A., Poedts, S., Huysmans, G. T. A. and Kerner, W. 1993 *Plasma Physics and Controlled Fusion* **35**, B277.

Goedbloed, J. P. and Poedts, S. 2004 *Principles of Magnetohydrodynamics, with Applications to Laboratory and Astrophysical Plasmas*, to appear (Cambridge University Press).

Goedbloed, J. P. and Sakanaka, P. H. 1974 *Phys. Fluids* **17**, 908.

Goedbloed, J. P. 1984 *Physica* **12D**, 107.

Goedbloed, J. P., Beliën, A. J. C., van der Holst, B. and Keppens, R. 2004 *Phys. Plasmas* **11**, 28.

Goossens, M., Andries, J. and Aschwanden, M. J. 2002 *Astron. Astrophys.* **394**, L39.

Hain, K. and Lüst, R. 1958 *Z. Naturforsch.* **13a**, 936.

Hameiri, E. 1981 *J. Math. Phys.* **22**, 2080.

Huang Y.-M. and Hassam, A. B. 2001 *Phys. Rev. Lett.* **87**, 235002.

Keppens, R., Casse, F. and Goedbloed, J. P. 2002 *ApJ* **569**, L121.

Kerner, W. and Lerbinger, K. 1985 *Comput. Phys. Commun.* **36**, 225.

Lortz, D. and Spies, G. O. 1984 *Phys. Lett.* A **101**, 335.

Lubow, S. H. and Spruit, H. C. 1995 *ApJ* **445**, 337.

Mahajan, S. M., Ross, D. W. and Chen, G. L. 1983 *Phys. Fluids* **26**, 2195.

Nakariakov, V. M., Ofman, L., DeLuca, E. E., Roberts, B. and Davila, J. M. 1999 *Science* **285**, 862.

Newcomb, W. A. 1960 *Ann. Phys.* **10**, 232.

Newcomb, W. A. 1962 *Nucl. Fusion Suppl.* Part 2, 451.

Nijboer, R. J., van der Holst, B., Poedts, S. and Goedbloed, J. P. 1997 *Comput. Phys. Commun.* **106**, 39.

Pao, Y. P. and Kerner, W. 1985 *Phys. Fluids* **28**, 287.

Sakanaka, P. H. and Goedbloed, J. P. 1974 *Phys. Fluids* **17**, 919.

Spies, G. O. 1978 *Phys. Fluids* **21**, 580.

Suydam, B. R. 1958 *Proc. 2nd U.N. Int. Conf. on Peaceful Uses of Atomic Energy*, Vol. 31, p. 157. New York: Columbia Univ. Press.

Tassoul, J. L. 1978 *Theory of Rotating Stars*. Princeton: Princeton Univ. Press.

van der Holst, B., Nijboer, R. J. and Goedbloed, J. P. 1999 *J. Plasma Phys.* **61**, 221.

van der Holst, B., Beliën, A. J. C. and Goedbloed, J. P. 2000 *Phys. Plasmas* **7**, 4208.

Wang, C., Keppens, R. and Goedbloed, J. P. 2003 *J. Phys.* D **36**, 2255.